***Jörg Jungwirth***
***Dipl. Ing., Doctoral Student***
***Structural Concrete Laboratory***
***Swiss Federal Institute of Technology (EPFL)***
***Lausanne, Switzerland***

***Aurelio Muttoni***
***Prof. Dr.***
***Structural Concrete Laboratory***
***Swiss Federal Institute of Technology (EPFL)***
***Lausanne, Switzerland***

# Structural Behavior of Tension Members in UHPC

**Summary**

The paper presents a study on the tensile behavior of UHPC conducted at the structural concrete laboratory at the Swiss Federal Institute of Technology in Lausanne (EPFL). Material tests and tests on structural members with reinforcement bars have been performed. A schematic representation of the material behavior allows a general description of the behavior of structural members in tension. The mechanical behavior for tension members and a simple model are presented.

Keywords: UHPC, tensile behavior, bond, structural members, conventionally reinforced UHPC elements, large scale testing

## 1 Introduction

The high performance concrete project currently under way at the Structural Concrete Laboratory (IS-BETON - EPFL) aims at examining new concept and design approaches to design statically efficient and economically viable structures using ultra high performance concrete.

In this scope, the scientific approach chosen is first to characterize and understand the behavior of UHPC by means of various laboratory experiences on material specimens and structural elements [1, 2]. On this basis, physical models are subsequently developed to describe the observed behavior. Finally, design concepts are proposed, with a perspective on potentially efficient structures.

The present paper focuses on the study of the behavior of UHPC in tension with and without conventional reinforcement. A series of tests on the tensile behavior of UHPC and the behavior of bar reinforced tension members in UHPC have been carried out and the main results are presented.

## 2 Material

The UHPC used for the tests is the CERACEM (BFM – Millau), provided as a premix. Its composition is given in table 1. The CERACEM (BFM – Millau) belongs to the BSI®/CERACEM range developed by SIKA and EIFFAGE [3]. The material is characterized by a relatively coarse composition compared to other UHPCs. Aggregates up to 7 mm are included in the matrix. The diameter of the added fibers of 0.3 mm is also relatively thick.

Table 1: Composition of the UHPC

| **Components** | | **Quantity** |
|---|---|---|
| Premix (cement, silica fume, sand and granular 0 - 7 mm) | kg/m³ | 2355 |
| Steel fibers ($l_f$ = 20 mm, $\varnothing_f$ = 0.3 mm, $\rho_f$ = 2.5 vol. %) | kg/m³ | 195 |
| SIKA specific superplasticizer | kg/m³ | 44.6 |
| Water | kg/m³ | 195 |

To obtain a reliable performance, a strict mixing procedure has to be followed. The batches are mixed in a high performance vertical axis mixer. For curing, the specimens are covered with a plastic foil after casting to avoid drying out. The formwork is taken off after 3 days and the specimens are stored under water until testing. Quality controls on hardened concrete were performed systematically in order to guarantee constant performance of the UHPC. All the tests were performed at 28 days.

## 3 Material behavior

To take into consideration the local effects of the crack opening, the tensile behavior of the material was analyzed through two different test series. Specimens with constant sections are used to study the uniformly distributed behavior until the crack opening. The local effects of the crack opening are investigated with notched specimens.

### 3.1 Distributed deformation

The tension tests are carried out on dogbone shaped specimens, with a length of 700 mm, a thickness of 45 mm and a width of 160 mm in the measurement zone (figure 1). The test is performed as a tension test on a clamped specimen. The specimen is fixed with glue in the support to avoid eccentricity and rotation [4]. The test is conducted at a constant deformation speed of 0.33 mm/min. The deformation is measured by 4 LVDT (linear variable differential transformer) on the front side and 5 strain gages on the back side.
In order to analyze the contribution of the two components (cement matrix and fibers), both fiber reinforced specimens and non fiber reinforced specimens are tested.

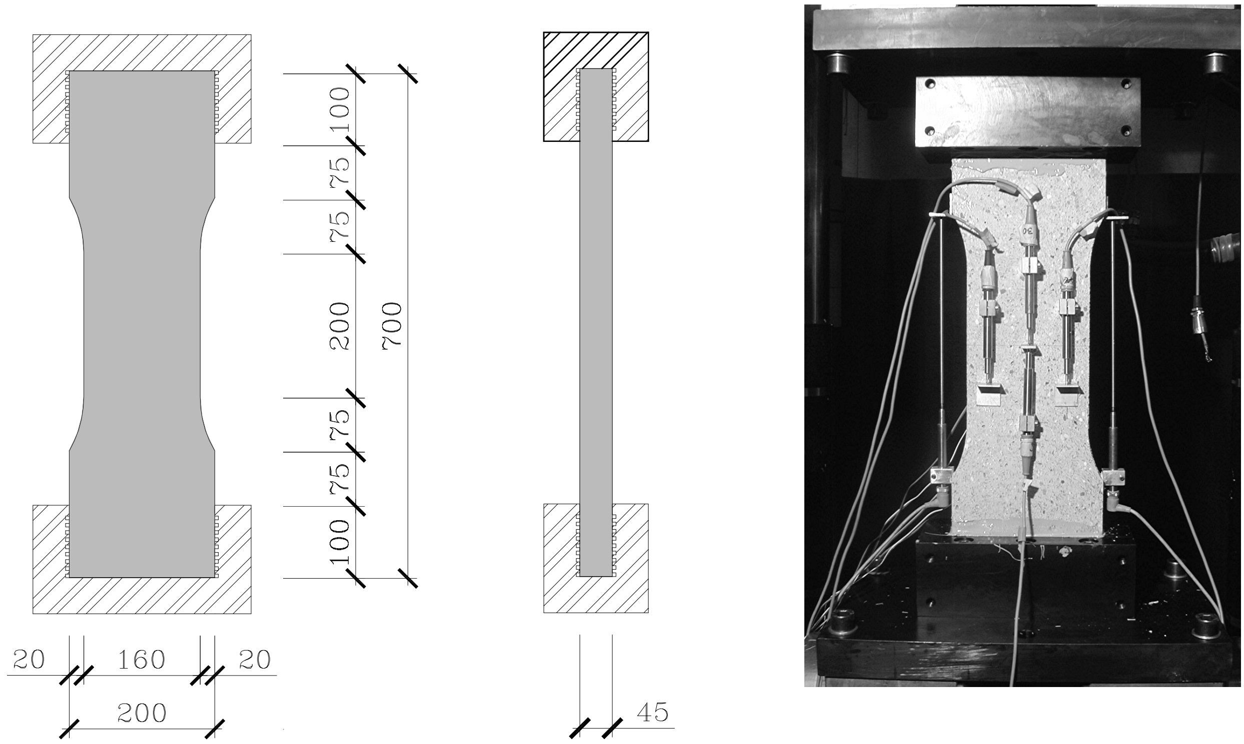


a) front view b) side view c) specimen during testing

Figure 1: Dogbone shaped specimen for the tensile test (dimensions in mm)

Two test series, with and without fibers, were carried out. Figure 2 shows the resulting stress-strain diagram. Both, the fiber reinforced specimens 1 & 2 as well as the specimen 3 (without fibers) show initially a linear elastic behavior with a Young's modulus of about 60 GPa (secant modulus 0 to 1/3 $f_{ct}$). At this stage, the fibers have almost no influence and the behavior is governed by the cement matrix. When the mean stress reaches a value of about 8.5 MPa, an initial crack appears. For the specimen without fibers (specimen 3), this leads to brittle failure. However, the stress of the fiber reinforced specimens 1 and 2 slightly increases up to 10 MPa. This effect is due to the high fiber ratio. The fibers crossing the crack have in total a higher strength than the cement matrix. The behavior is similar to the traditional reinforced concrete, characterized by an increase of the capacity after cracking. During this stage multiple cracks are created. This multi cracking effect is regularly distributed over the whole length of the specimen, so it can be assumed as smeared. The very small crack opening (micro-cracks) is just large enough to activate the fibers allowing the transfer of the stresses from the matrix. At a strain of about 2.5 ‰, all cracks have been formed and the bond strength of the fibers crossing the crack is reached in one of the cracks. The deformation localizes in this crack, which opens to become a macro-crack. Finally the fibers are progressively pulled out.

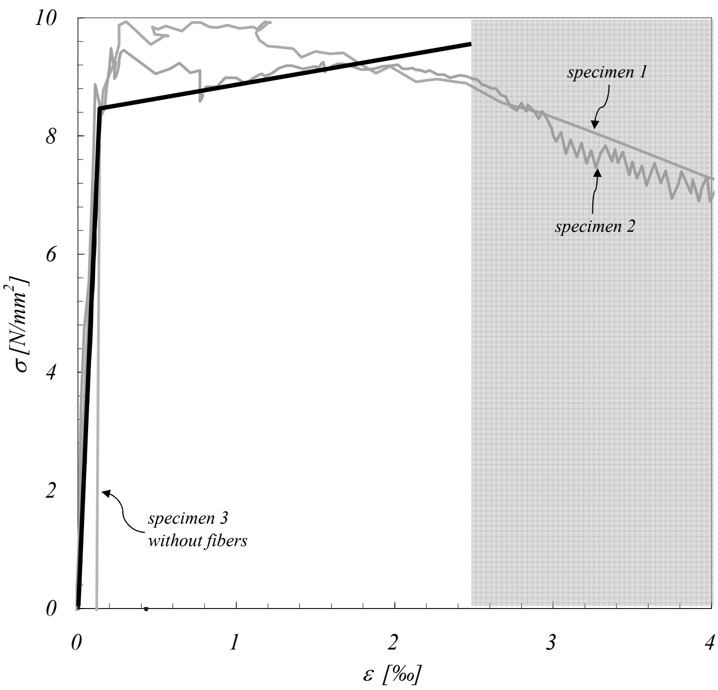


a) stress – strain diagram

| | $E$ [GPa] | $f_{ct,matrix}$ [MPa] | $\varepsilon_{matrix}$ [‰] | $f_{ct}$ [Mpa] | $\varepsilon_t$ [‰] | note |
|---|---|---|---|---|---|---|
| **1** | 63 | 8.8 | 0.16 | 9.9 | 2.5 | |
| **2** | 66 | 8.9 | 0.11 | 9.5 | 2.5 | |
| **3** | 60 | 7.8 | 0.14 | - | - | no fibers |

b) results

Figure 2: Pre-peak behavior of the tested UHPC

Several authors propose a bi-linear relation as shown in figure 2 to approximate the behavior of UHPCs [5, 6]

1. The elastic behavior of the matrix described by the Young's modulus and the tensile strength of the matrix.
2. A linear approximation of the multi-cracking phases up to the ultimate bond strength of the fibers crossing the crack.

For the tested UHPC, where the difference between the matrix strength and the ultimate strength is quite small, a linear approach in the multi-crack stage may not be ideal. As the small number of specimens doesn't allow a detailed analysis, the bi-linear relation is adopted as a first approach.

The crack spacing in the multi-crack stage can be estimated by the approach used for traditional reinforced concrete. With the assumption that the force in the fibers (length $l_f = 20\,mm$) crossing the crack is completely transferred to the matrix over the distance of $l_f/2$, the maximal crack spacing is $s_{\max} = 2 \cdot l_f/2 = 20\,mm$. If there are two cracks with a spacing larger than the maximum distance, another crack will appear. Thus, the minimal crack spacing is $s_{\min} = l_f / 2 = 10\,mm$. So the average crack spacing can then be estimated as

$$s_r = \frac{3}{4} l_f = 15\ mm \tag{1}$$

which corresponds well to the crack-spacing observed on the specimens.

### 3.2 Crack opening

The crack opening behavior of the UHPC after the formation of the macro crack can be observed by means of a notched tensile test (see figure 3). The cross section of the specimen is weakened to a width of 160 mm by a sawed notch in order to control the crack formation. Otherwise, the rest of the test setup is the same as for the previous test. The development of the crack is observed with strain gages on the backside and the crack opening is measured with two LVDTs on the front side of the specimens. The crack is initiated over the whole width of the section by several pre-loading cycles. The pre-loading cycles were started with a nominal stress of 5 MPa. At every subsequent cycle the peak force was increased by 0.5 MPa until the strain gage located over the crack on the backside of the specimen showed the initiation of the crack opening. Subsequently, the crack opening was conducted in one load cycle with a constant deformation speed of 0.08 mm/min.

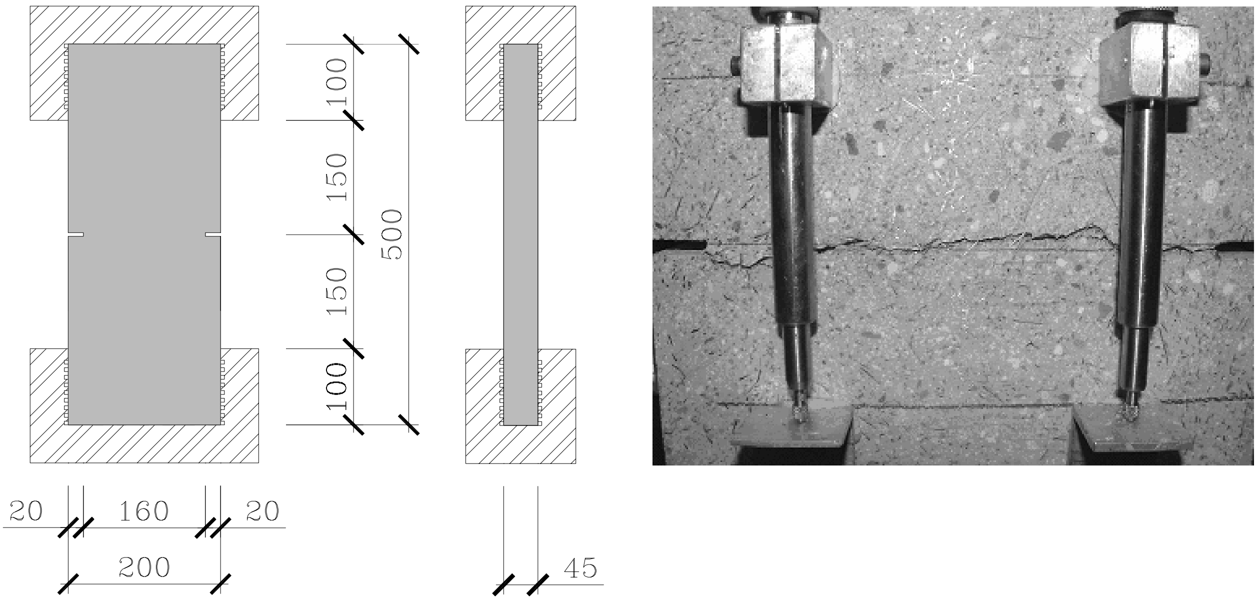


a) front view b) side view c) specimen during testing, opened crack

Figure 3: Notched specimen for the tensile test (dimensions in mm)

In order to obtain the actual crack opening from the measurement, which covers a length of 100 mm, the contribution from the uncracked parts of the specimens must be deducted. Elastic uncracked behavior can be assumed, because the stress level remains below the strength of the matrix in the intact part of the specimen. Figure 4a shows, for the three tested specimens (specimen 4, 5, 6), the average stress versus crack opening diagram inserted in the stress – displacement diagram of the test.

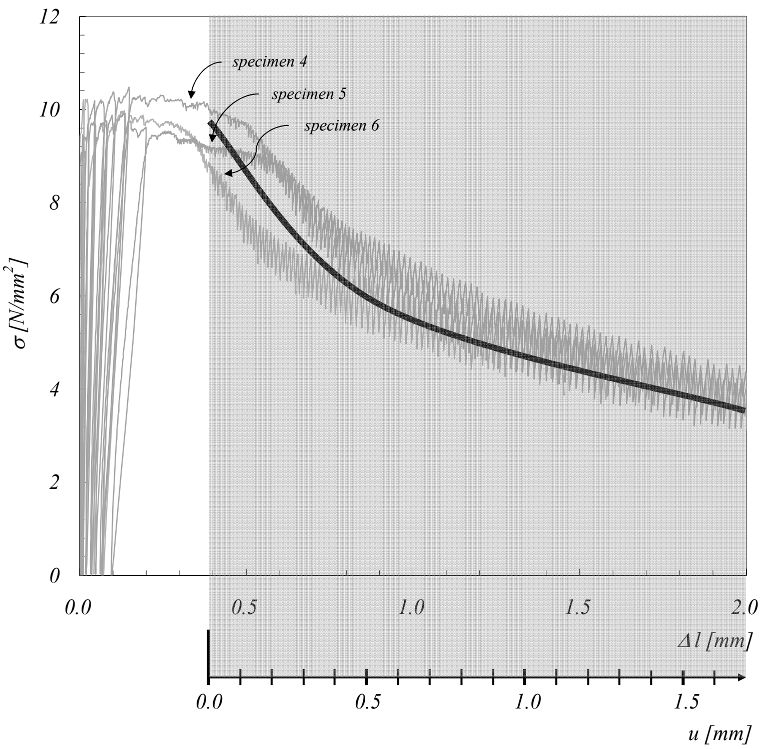


a) crack opening behavior b) pulled out fibers

Figure 4: Crack opening behavior of the notched specimens

The crack opening is accompanied by a decrease of the mean axial stress. The decrease of the stress is initially large and becomes smaller for larger crack openings. The fracture surface shows that all the fibers are pulled out and that none of them breaks by reaching its ultimate strength (figure 4b).

## 3.3 Tensile behavior of an UHPC element

The tensile behavior of a tensile element of arbitrary length can now be derived from the distributed pre-peak behavior and the local crack-opening behavior. In a stress-strain diagram (figure 5) the elastic phase (phase 1) and the multiple micro-cracking phase (phase 2) are independent from the length of the specimen. The multi-cracking is a well distributed phenomenon assumed to be smeared over the length. During the multi-cracking phase the fibers are activated when the micro-cracks open. When the ultimate bond stress of the fibers crossing the crack is reached in one crack, the fibers are progressively pulled out. This results in a concentration of the deformation in this particular crack. The nominal strain of the element due to the crack opening (phase 3) thus depends on the length of the element.

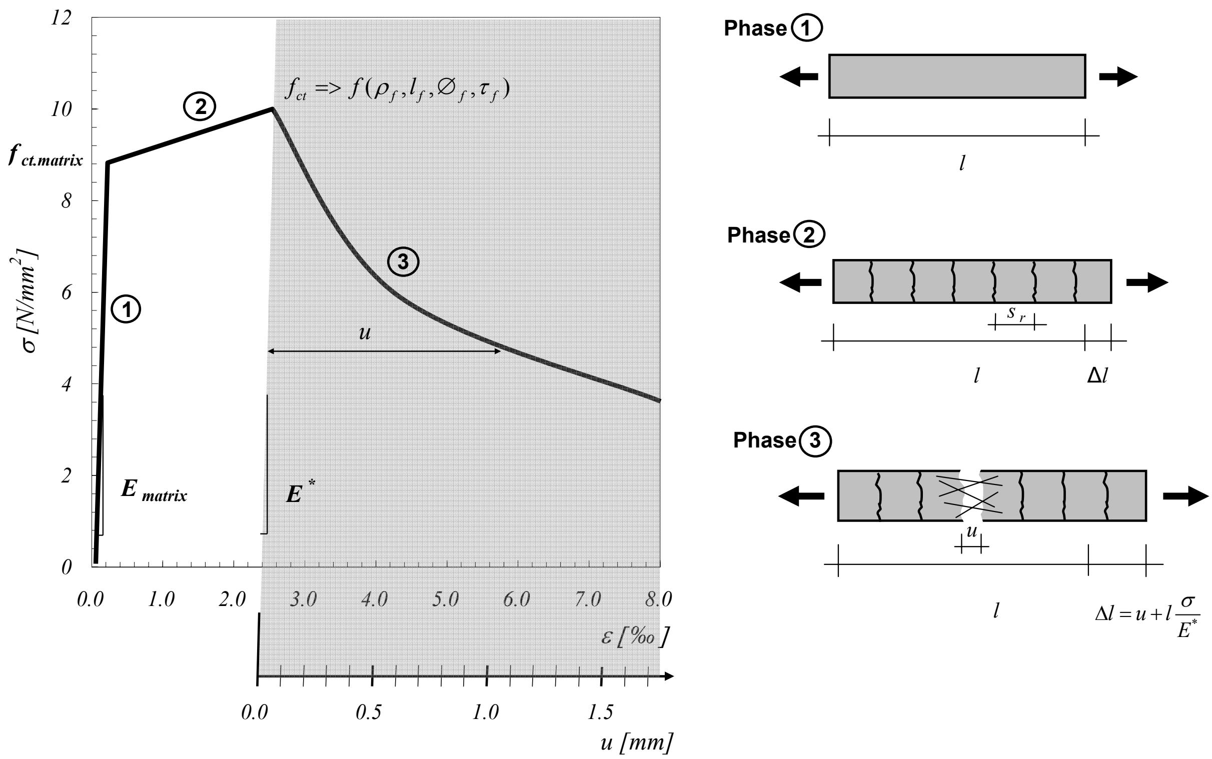


a) stress-strain diagram

b) schema of the multi-cracking phase and crack localization

Figure 5: Schematic behavior of a UHPC tensile element

The deformation can be calculated according to the fictive crack model by Hillerborg [7] as the sum of the crack opening $u$ and the elastic deformation of the rest of the element (equation 2). $E^*$ is the unloading modulus, depending on the stiffness of the matrix and the total elastic deformation of micro cracks (not discussed in this paper).

$$\Delta l = u + l\frac{\sigma}{E^*} \tag{2}$$

For various types of UHPC, the shape of the graph is basically the same [4, 5, 6, 8]. The gradient and the length of the different phases vary slightly depending on the composition of the UHPC. The elastic phase is governed directly by the characteristics of the cement matrix ($f_{ct,matrix}, E_{matrix}$). Phases 2 and 3 are governed by the length, the diameter and the ratio of the fibers and by the bond behavior between fibers and the matrix.

## 4 Structural members

The characteristics of a structural member in tension can be analyzed based on the material behavior illustrated above. In order to obtain an efficient and reliable tie element, it might be reasonable to use fiber reinforced UHPC in combination with steel reinforcement. This is why the bond between reinforcement and the UHPC is analyzed next.

### 4.1 Bond of reinforcement bars

The bond between reinforcement bars and the fiber reinforced cement matrix is investigated by means of a reinforcement bar pullout test. Knowledge of the bond strength enables to determine the development length and the crack spacing.

The specimen consists of a 160 mm cube with a reinforcement bar (GEWI) positioned in the center (figure 6a). Six specimens with different bond lengths $l_b$ ranging from 20 to 50 mm and two different bar diameters (12 and 20 mm) are tested.

The specimen is loaded by pulling on the reinforcement bar. A metal plate with a central hole serves as support. The slip is measured on the upper side of the specimen as the relative displacement of the bar's end and the concrete surface.

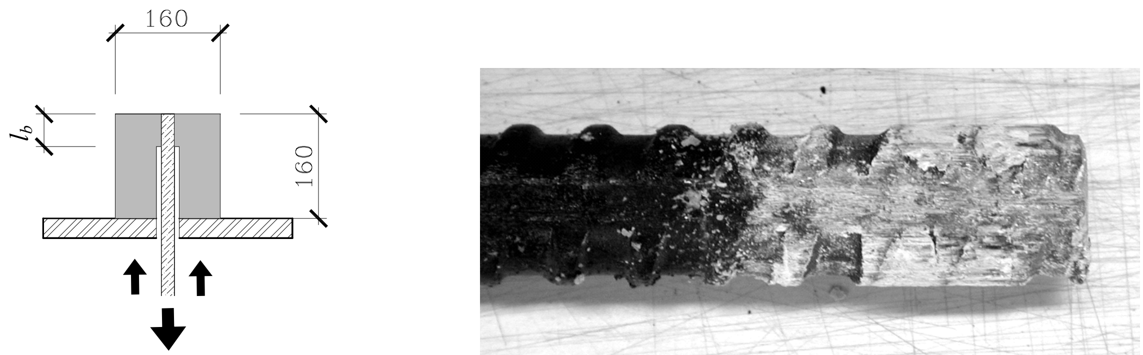


a) test setup b) pulled out bar

Figure 6: Pullout test (dimensions in mm)

As one can see in figure 6b, the fracture occurs by shearing of the cement matrix. The sheared concrete still sticks between the ribs.

Figure 7 shows the bond-slip-relationship for two different bar diameters (∅12 mm and ∅20 mm). Further, the yield stress and the tensile strength of the bars are indicated.

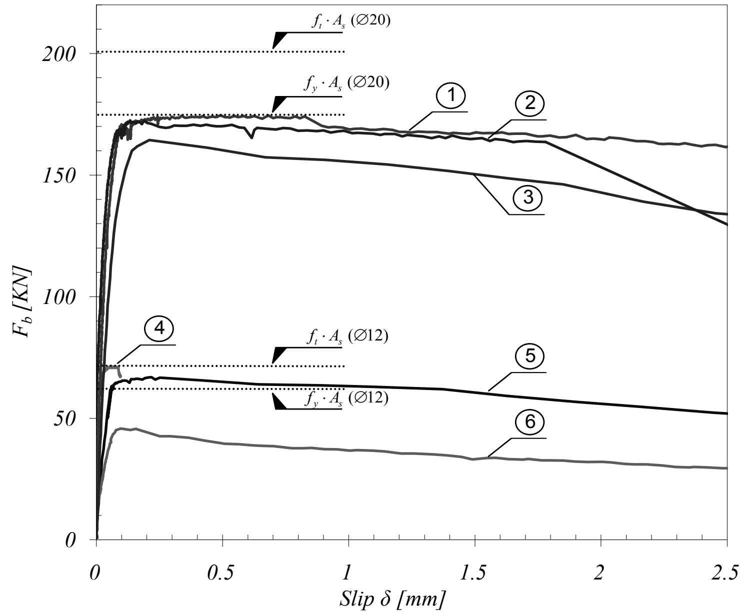


a) force – slip diagram

| | ∅ [mm] | $l_b$ [mm] | $A_b$ [mm²] | $F_b$ [KN] | $\tau_b$ [MPa] | note |
|---|---|---|---|---|---|---|
| 1 | 20 | 50 | 3140 | 174 | 55 | yielding |
| 2 | 20 | 50 | 3140 | 171 | 54 | - |
| 3 | 20 | 40 | 2512 | 165 | 66 | - |
| 4 | 12 | 50 | 1880 | >71 | >38 | bar strength |
| 5 | 12 | 30 | 1128 | 67 | 59 | yielding |
| 6 | 12 | 20 | 752 | 46 | 61 | - |
| average bond strength (without 4): | | | | | **59** | |

b) results

Figure 7: Results of the pullout tests (slip at the unloaded end)

In a first phase the behavior is almost linear. Once the bond strength is reached, the slip increases while the force decreases due to the reduced bond length and a non ductile behavior. In the specimen 4 ($\varnothing = 12\ mm,\ l_b = 50\ mm$) the bar strength of the reinforcement has been reached because of a very long anchorage length.

Assuming a constant bond stress distribution, the bond strength can be calculated as the ratio of the pullout strength and the bond surface:

$$\tau_b = \frac{F_b}{\varnothing \pi l_b} \tag{3}$$

The average value of the tested specimens is: $\tau_b = 59\ MPa$

This bond strength is about 10 times higher than the bond strength of conventional concrete.

The theoretical development length is thus much shorter and can be calculated as:

$$l_b = \frac{f_y \varnothing_S}{4\tau_b} = 2.4 \cdot \varnothing_S \tag{4}$$

## 4.2 Tensile behavior of bar reinforced members

In order to understand the behavior of structural members in UHPC, large scale tests simulating the condition in actual structures have been carried out.

Three specimens with different reinforcement ratios between 1 % and 4.8 % (ribbed steel, $f_y$ = 556 MPa) have been tested. The dimensions of the specimens are 160 x 160 x 1500 mm with a measurement length of 1000 mm (figure 8a/b). The strain is measured all along the measurement zone with extensometers spanning over 100 mm.

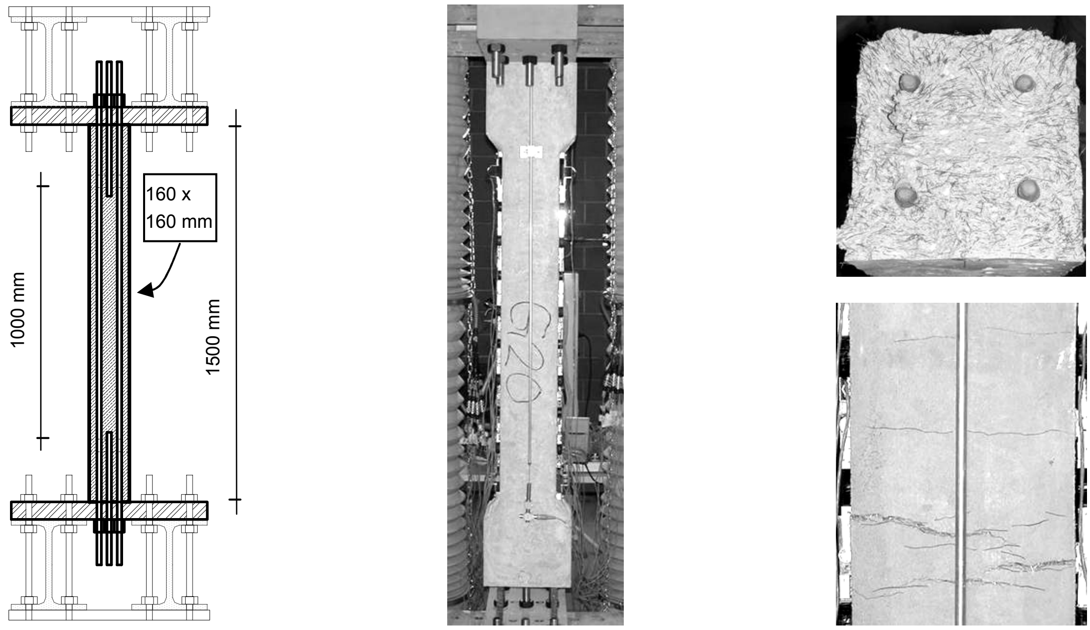


a) test setup  b) front view  c) specimen after testing

Figure 8: Tensile test of structural members

The tested specimens show a multi cracking behavior (figure 8c). On the fracture surfaces, the fibers that have been pulled out and the plastic deformation of the reinforcement bars can be observed.

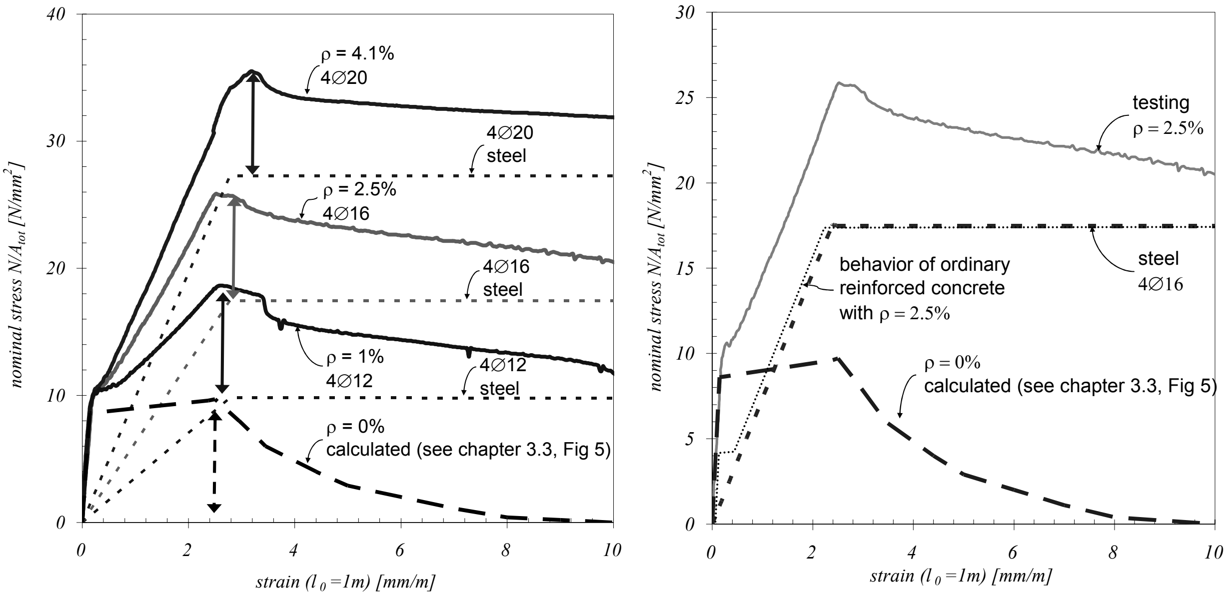


a) different reinforcement ratios

b) comparison with model for ordinary reinforced concrete (4∅16)

Figure 9: Stress – strain diagram of the tests on bar reinforced structural members in UHPC

The nominal stress - strain diagram for the three different reinforcement ratios ($\rho$ = 1 %, 2.5 % and 4.5 %) is shown in figure 9a (measurement length 1000 mm). The steel behavior for the three cases and a calculated curve for an unreinforced specimen are given for comparison. Figure 9b focuses on the specimen reinforced with 4∅16 and compares the measured behavior of the UHPC with the model for the behavior of ordinary reinforced concrete.
It can be observed, that unlike in the case of ordinary concrete, the strength is composed of the steel strength and a contribution of the UHPC. The contribution of the concrete to the stiffness of the element (tension stiffening) is very high due to the very high bond and tensile strength.

## 5 Conclusion

Due to the fibers and their contribution to the behavior in tension UHPC shows a different tensile behavior than ordinary concrete. This has an important influence on the design of structures in UHPC. It can be concluded that:

- Major tension stresses should be taken by reinforcement bars or pre-stressed steel to guarantee a reliable and efficient tension bearing.
- The strain hardening effect caused by the fibers leads to a well distributed multi cracking. This eliminates the need of minimal reinforcement for crack distribution.
- The good bond between reinforcement and the matrix leads to a short development length. This should make connection of precast elements very easy.
- Shear reinforcement and reinforcement for the punching zones are not needed for minor shear stresses due to the high tensile strength respectively the high shear strength.

This means that structures can be designed only with UHPC and pre-stressing cables or passive reinforcement carries the major tensile stresses. No further reinforcement is needed.

One possible application of UHPC in tension is its utilization as tendon in underspanned girders (figure 10) [9]. Due to high compression strength of the UHPC a high pre-stress ratio with a high pre-stress force can be employed. This tendon has a very high cracking limit and will remain very stiff after cracking due to the fiber reinforcement. The small crack spacing and the small crack opening should make this tendon also very durable.

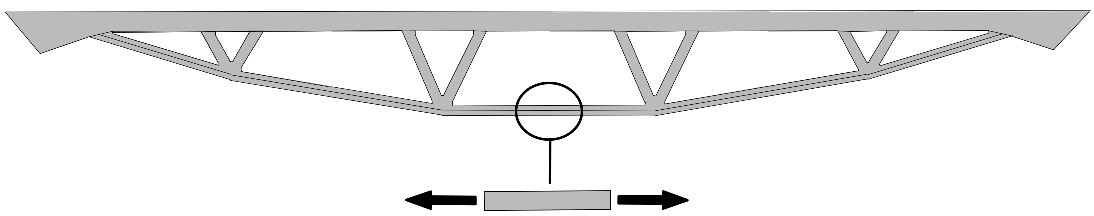

Figure 10: Tensile members for underspanned structures (longitudinal section)

## 6 Acknowledgements

The research project 'ultra high performance concrete' at IS-BETON-EPFL in which context the presented studies were carried out, is kindly supported by CEMSUISSE.

The UHPC was a friendly donation from the companies EIFFAGE and SIKA and the pre-stressing strands and equipment a kind donation from VSL.


## 7 References


[1] **Jungwirth J., Muttoni A.,** *Versuche an Bauteilen aus ultrahochfesten Beton – Teil 1 Material,* EPFL-IS-BETON, Lausanne, **2004**

[2] **Jungwirth J., Muttoni A.,** *Versuche an Bauteilen aus ultrahochfesten Beton – Teil 2 Bauteile*, EPFL-IS-BETON, Lausanne, **2004**

[3] **Maeder U., Lallemant – Gamboa I., Chaignon J., Lombard J.P.,** *CERACEM a new high performance concrete : characterization and applications*, Conference on the UHSC, Kassel, **2004**

[4] **Habel K., Gysler R., Denarié E., Brühwiler E.,** *A Uniaxial Tensile Test for Advanced Cementitious Materials*, internal report, 8 p., **2002**

[5] **Behloul M.**, *Analyse et modélisation du comportement d'un matériau à matrice cimentaire fibrée à ultra hautes performances*, E.N.S. Cachan, doctoral thesis, 182 p., Cachan, France, December, **1996**

[6] **SETRA, AFGC** , *Béton fibrés à ultra-hautes performences*, recommandations provisoires, p. 152, France, **2002**

[7] **Hillerborg A.**, *Analysis of a single crack*, Fracture mechanics of concrete edited by F.H.Wittmann, Elsevier science Publishers B.V., pp 223-249, Amsterdam, Hollande, **1983**

[8] **Plumey S., Jungwirth J., Muttoni A.**, *Comportement des éléments en béton à ultra hautes performances*, EPFL-IS-BETON, Lausanne, **2002**

[9] **Muttoni A.,** *Innovationen im Brückenbau am Beispiel der unterspannten Tragwerke*, Internationales Brückensymposium, Darmstadt, **2003**